

# Characterization of Various Sn Targets with Respect to Debris and Fast Ion Generation

Yoshifumi Ueno, Hideo Hoshino, Tatsuya Ariga, Taisuke Miura, Masaki Nakano, Hiroshi Komori, Georg Soumagne, Akira Endo, Hakaru Mizoguchi, Akira Sumitani and Koichi Toyoda  
EUVA (Extreme Ultraviolet Lithography System Development Association),  
1200 Manda Hiratsuka, Kanagawa, 254-8567, Japan

## ABSTRACT

We evaluated Sn debris generated from a CO<sub>2</sub> laser (10.6 $\mu$ m) and a Nd:YAG laser (1064nm) plasma. Experiments were performed with bulk Sn-plates (t=1mm) and freestanding Sn-foils (t=15 $\mu$ m). Quartz Crystal Microbalances (QCM) were used for debris analysis. We observed a drastically lower deposition for the CO<sub>2</sub> laser driven plasma compared with the Nd:YAG laser plasma. In addition, several Sn coated targets with different Sn thickness were investigated for the CO<sub>2</sub> drive laser with respect to the generated plasma debris. In general, a 100nm Sn coated glass target generated more debris than the solid Sn target. Especially, we observed for the Sn-plate target that the deposition rate is smaller than the erosion (sputter) rate caused by the plasma ions.

**Keywords:** Extreme Ultraviolet Lithography, Laser Produced Plasma, Debris, Deposition, Erosion

## 1. INTRODUCTION

The target material of choice for EUVL plasma light sources is Sn due to its high conversion efficiency. Its main drawback, however, is the generated debris that severely limits the lifetime of the EUV collector mirror (and other optical) components. In general, the Sn debris from the laser-produced plasma consists of energetic plasma ions and neutrals, evaporated material, and liquid droplets, which solidify when they deposit on a surface. The latter, i.e. the ejected droplets, are typical debris particulates of a Sn target because tin is not a gas like Xe. In general, the generated Sn debris greatly reduces the EUV collector mirror lifetime via deposition (evaporated material, molten droplets, slow ions /neutrals), erosion (fast ions/neutrals), and implantation (ultra fast ions/neutrals).

A plasma consists of neutrals, electrons and ions. The charged particles can be mitigated by electric or magnetic fields. This was experimentally confirmed, especially the effect of magnetic field mitigation<sup>1,2</sup>. Neutral particles can evidently not be controlled by electric or magnetic fields but by the target layout and the laser irradiation method. Ideally, a fully ionized plasma is generated based on a mass limited target, which is in practice, however, very difficult.

The amount of Sn that is allowed to deposit on the collector mirror is very small. Already a Sn thickness of about 1nm, i.e. only several atomic layers, reduces the mirror reflectivity by 10% which is commonly regarded as the mirror lifetime specification. On the other hand, the acceptable erosion depends on the Mo/Si multilayer number of the mirror. Taking sacrificial layers into account the total layer thickness is of  $\mu$ m order. Hence, the debris deposition is more critical than the layer erosion and has to be addressed first.

Mitigation of debris deposition has been attempted by several methods. The usage of low-pressure (0.2Torr, He) background gas was successful to reduce the deposition of small particles (<0.3 $\mu$ m).<sup>3,4</sup> Larger particles (>0.5 $\mu$ m), however, cannot be stopped by the low-pressure background gas.<sup>5,6</sup> This requires a higher gas pressure, which, on the other hand, causes significant absorption of the generated EUV light. Especially, the mitigation of molten debris with still larger size and mass is not yet established and, although various debris studies have been made with a Nd:YAG drive laser, little is known about CO<sub>2</sub> laser generated debris. Therefore, we investigated deposition characteristics of various Sn targets irradiated with a CO<sub>2</sub> laser.

## 2. EXPERIMENTAL SETUP

A schematic of the experimental set-up is shown in figure1.

The Sn target is placed at the center of the vacuum chamber at an angle close to 0deg related to the incident laser beam. The laser beam is focused onto the target with a  $f=60\text{mm}$  lens. The resulting minimum spot size is estimated to be  $100\mu\text{m}$  fwhm. The vacuum pressure during experiments is about  $10^{-3}\text{ Pa}$ , i.e. the transmission at  $13.5\text{nm}$  is practically 1. A Flying Circus 2 EUV energy meter is placed at  $60\text{deg}$  related to the laser beam axis to measure the generated in-band energy.

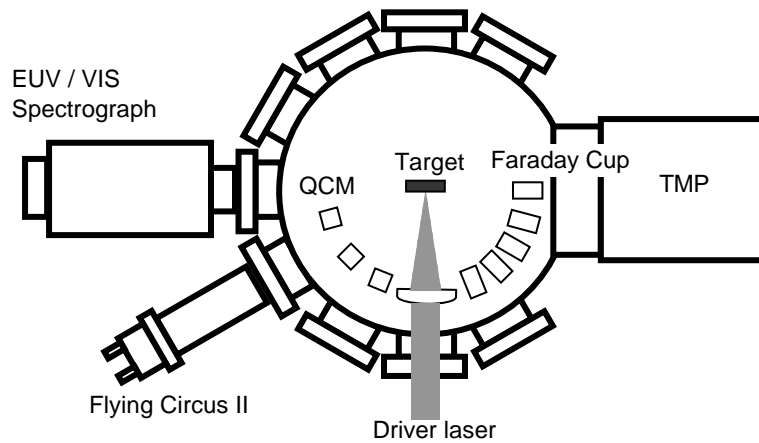


Fig. 1. Schematic of the experimental set-up.

Figure.2 shows the placement of the instruments inside the vacuum chamber. The QCM and Faraday cups for debris and ion analysis, respectively, were symmetrically placed at a distance of  $100\text{mm}$  from the plasma. The QCM used gold coated quartz crystals and deposition/erosion was monitored real time with a QCM controller (ULVAC, CRTM-9000).

All data, i.e. from the FC2 (EUV energy), the QCM (deposition/erosion), and the Faraday cup (ion), was taken simultaneously.

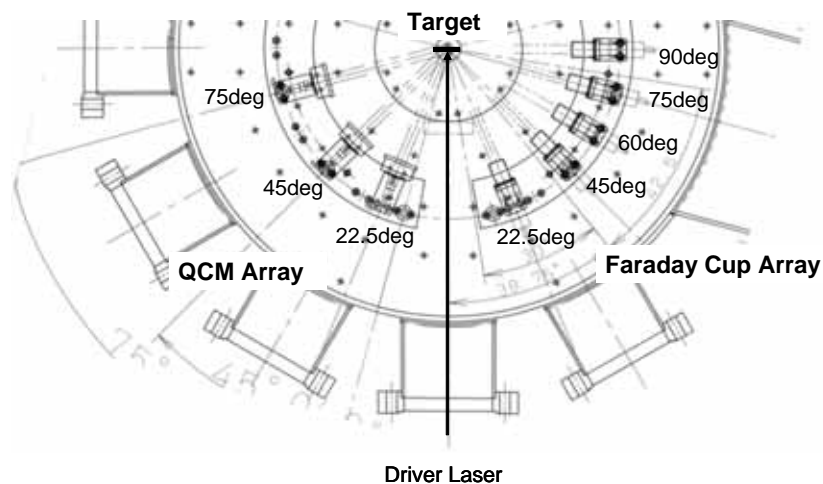


Fig. 2. The placement of the instruments inside the vacuum chamber.

A TEA-CO<sub>2</sub> master oscillator power amplifier (MOPA) laser system has been used as drive laser. The oscillator is based on a commercial unit that delivers 100ns pulses at a maximum repetition rate of 100Hz. It was modified with a Pockels cell and had a matched resonator length to generate 10ns pulses with a max. pulse energy of 3mJ. The pulse energy is amplified by passing the laser beam 3-times through a modified excimer laser unit from Gigaphoton Inc., i.e. the discharge chamber windows and discharge electrodes have been modified for CO<sub>2</sub> laser operation. A maximum amplification of 10 results in a max. pulse energy of 30mJ. In addition to the CO<sub>2</sub> laser, a Q-switched Nd:YAG laser at 1064nm (Spectra-Physics, Quanta-Ray INDY) was used for comparison.

### 3. EXPERIMENTAL RESULTS

#### 3.1 Debris evaluation with Nd:YAG drive laser

A typical QCM signal for the Sn-plate target is shown in figure3. The figure shows an increase of the Sn deposition versus time, which is almost linear to the laser shot number.

After 40s the laser was switched off and the QCM signal remains therefore constant.

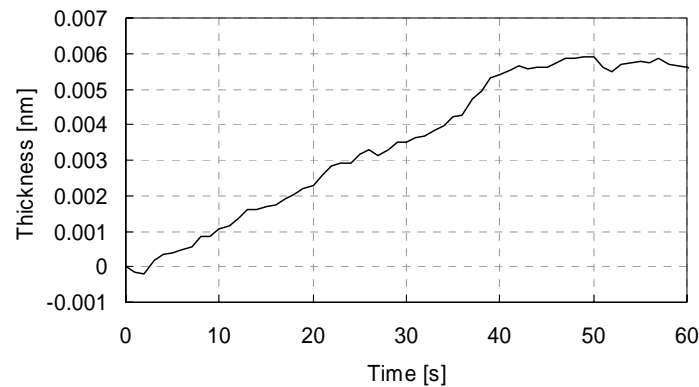


Fig. 3. A typical QCM signal for the Sn-plate target with Nd:YAG laser.

Figure.4 compares QCM results of the bulk solid Sn-plate with the freestanding Sn-foil target for different measurement angles. The vertical axis is the deposition rate per in-band EUV energy. The laser energy is 35mJ, the average EUV energy is 0.45mJ, i.e. the average CE is about 1.3%. Note that we observed no change of the deposition rate for at a ten times higher laser energy of 350mJ.

Deposition is observed at all angles, but the amount of deposition increases closer to the laser beam axis, i.e. closer to the target normal. Especially, the deposition rate for the Sn-foil target is only about 1 order lower than the Sn-plate deposition. This reduction is probably due to the mass limiting effect of the much smaller target thickness, i.e. in case of the Sn-foil target, a hole was “shot” into the foil after only one laser pulse. We suppose therefore that the generated heat and pressure of the plasma reaches a target depth of 15um or more, and that debris is mainly generated from deep inside the target material.

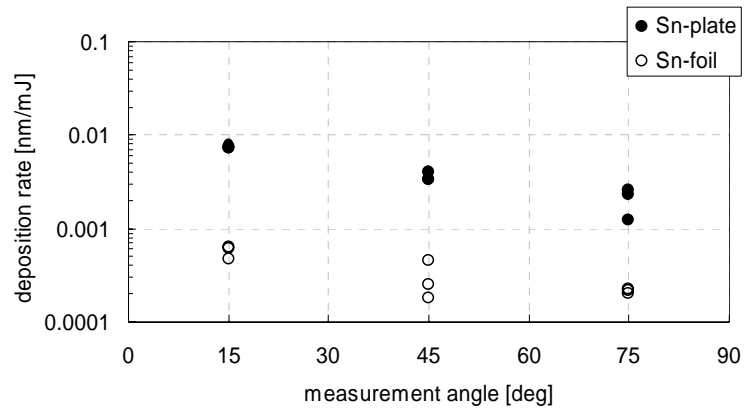


Fig. 4. QCM results of the solid Sn-plate and Sn-foil target for different measurement angles with Nd:YAG laser.

### 3.2 Debris evaluation with CO<sub>2</sub> drive laser

The experiments done with the Nd:YAG drive laser were repeated with the CO<sub>2</sub> drive laser to investigate the debris characteristics for different drive lasers.

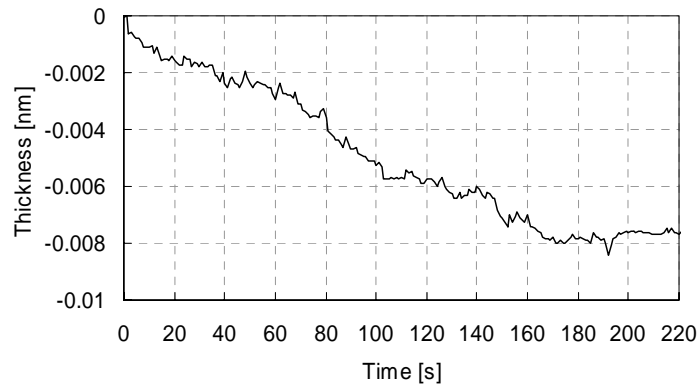


Fig. 5. A typical QCM signal for the Sn-plate target with CO<sub>2</sub> laser.

A typical QCM signal for the Sn-plate irradiated with the CO<sub>2</sub> laser is shown in figure5. After 170s the laser was switched off and the QCM signal remains therefore constant.

Contrary to the Nd:YAG laser, the Sn deposition now decreases with the laser shot number, i.e. the slope (or rate) is negative indicating erosion. The sputtering rate by fast ions/neutrals is therefore higher than the deposition rate by evaporated material, molten droplets and slow ions /neutrals.

Figure.6 compares the QCM results of the solid Sn-plate with the freestanding Sn-foil target for different measurement angles. The vertical axis is the deposition rate per in-band EUV energy. The laser average energy is 25mJ, the average EUV energy is 0.5mJ, i.e. the average CE is about 2.0%.

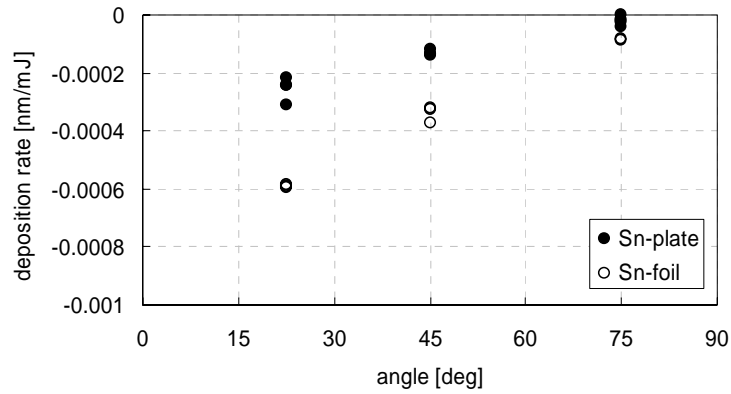


Fig. 6. The QCM results of the solid Sn-plate and Sn-foil target for different measurement angles with CO<sub>2</sub> laser.

Erosion, i.e. a negative deposition rate, is obtained at all angles, but it is larger for angles closer to the laser beam axis, which is due to the angular ion distribution. In addition, the erosion rate is slightly larger for the Sn-foil. This is probably due to a slight increase of the ion number and not a decreased deposition because for both targets the measured (single-shot) ablation depth is about 1µm but the measured ion signal is slightly larger for the Sn-foil target. Note that the laser always irradiates a fresh target surface, i.e. the target is continuously displaced between laser pulses. Hence, there is no mass difference between the 15µm foil and the 1mm target and a difference is only expected for a Sn target thickness below 1µm.

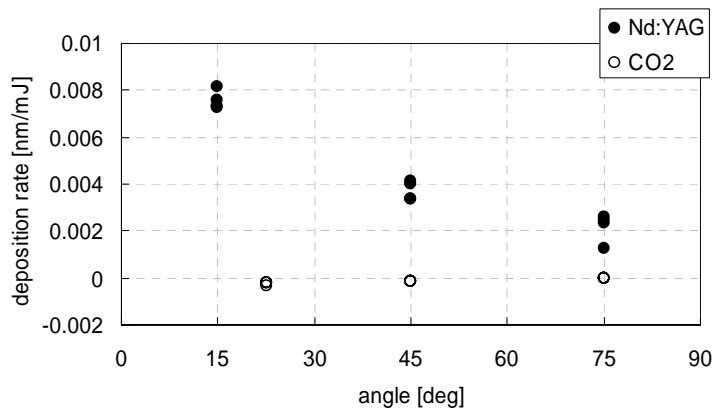


Fig. 7. Solid Sn-plate QCM results for Nd:YAG and CO<sub>2</sub> drive laser.

Figure.7 finally summarizes the Sn-plate results for the Nd:YAG and the CO<sub>2</sub> drive laser. The figure shows the sputter/deposition rate versus the observation angle.

### 3.3 Ion measurement

The ion waveform of the Nd:YAG and the CO<sub>2</sub> laser produced plasma of a Sn plate is shown in figure.8.

The ion signal has been measured with a Faraday cup placed inside the vacuum chamber. (see figure.2) At the same EUV in-band energy the ion waveforms are almost identical with respect to the peak and maximum ion energies. In addition, no major difference of the total ion signal, i.e. the integral value, is observed. This indicates that in both experiments the mean ion charge is identical as measured by an almost identical CE. Hence, for both lasers the sputtering by the generated ions is also almost identical.

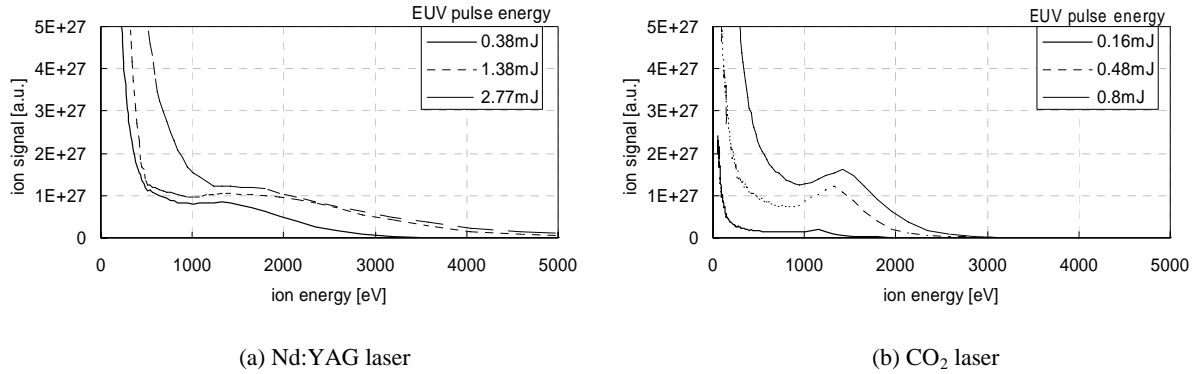


Fig. 8. Ion waveforms generated by the Nd:YAG and CO<sub>2</sub> laser.

It is not outlined in detail here, see e.g.<sup>1,2</sup>, but the ion signal of the Nd:YAG laser generated plasma decreased below the Faraday cup detection limit (about 3 orders) applying a magnetic field of 1T (see figure.9). The QCM signal, on the other hand, does not change applying a magnetic field between 0T and 1T as shown in figure.10. Hence, the ions only weakly influence the deposition. From the experimental results it is estimated that the effect is below 1%. In case of a Nd:YAG drive laser and a Sn target, debris mitigation is therefore much more important than ion mitigation.

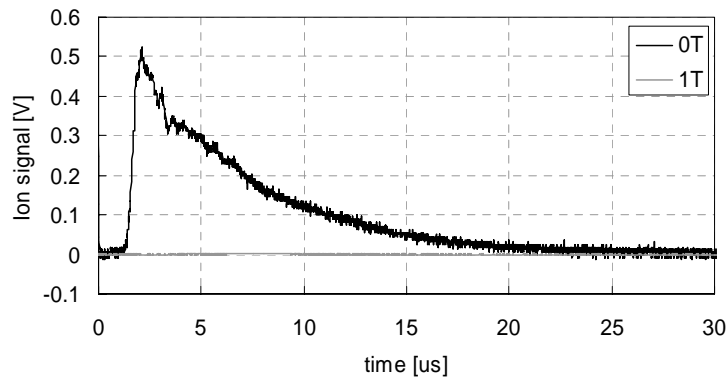


Fig. 9. The ion waveform generated by the Nd:YAG laser with/without magnetic field.

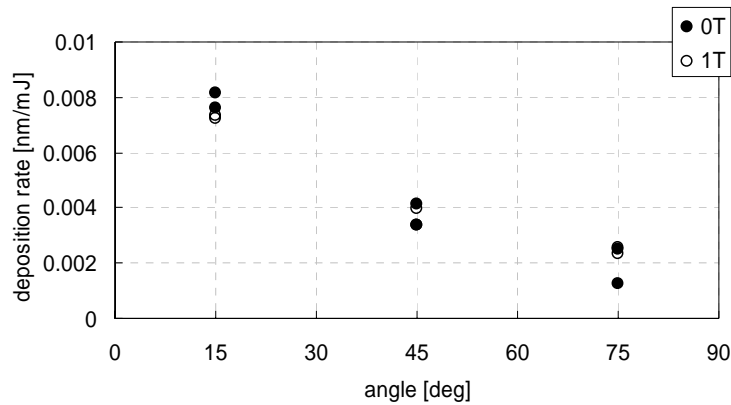


Fig.10. The QCM results for Nd:YAG laser with/without magnetic field.

### 3.4 Evaluation of various Sn targets with CO<sub>2</sub> drive laser

#### 3.4.1 QCM result

For a solid Sn plate irradiated with the CO<sub>2</sub> laser very little debris is generated. We also evaluated targets like Sn coated copper and glass substrates to investigate the mass limiting effect for various Sn thicknesses. Note that the same CE has been obtained for all targets. Figure.11 summarizes the QCM results of these targets as a function of the Sn thickness. Dots show the Sn plate results and circles the Sn coated glass substrate (Sn thickness from 0.1 to 0.01 $\mu$ m) and Sn coated Cu tape results (Sn thickness of 4 $\mu$ m).

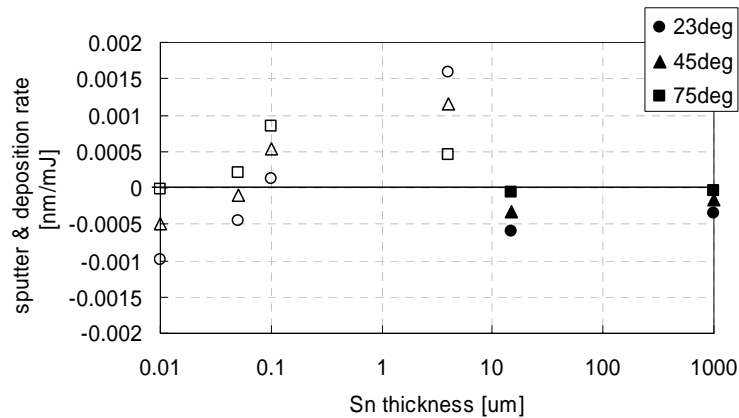


Fig.11. QCM results of various Sn targets as a function of the Sn thickness.

As already mentioned, erosion is observed for the 1mm Sn-plate and the 15 $\mu$ m Sn-foil. The 4 $\mu$ m Sn coated Cu tape and the 100nm Sn coated glass, however, show deposition. The difference can be explained with the melted area observed on the target surface. For the Sn plate a melted target area of 200  $\mu$ m diameter was observed after laser irradiation. On the other hand, for the coated targets, the Sn layer was completely removed within a diameter of about 1mm. This is probably due to differences in thermal conductivity, shock (blast) wave generation and/or adhesion, but is currently not fully understood. Note that the measured deposition rate decreases with decreasing Sn coating thickness and that below 100 $\mu$ m the QCM signal shifts from deposition to erosion.

### 3.4.2 Si WitnessPlate Result

In order to confirm the QCM measurements Si witness plates were used to sample the deposition. The Si plates were placed at the Faraday cup positions; see Figure.2. A Sn-plate (erosion) and a 800nm Sn coated glass substrate (deposition) were used as targets. Figure.12 shows the QCM result for both targets, and figure.13 shows optical microscope images of the Si witness plates. Both measurements show very good agreement. For measured QCM deposition (Sn-coat target), Sn particles were observed on the Si witness plate. No Sn particles were observed for slight QCM erosion (Sn-plate target). This is only a preliminary analysis and samples will be analyzed in more detail in the near future.

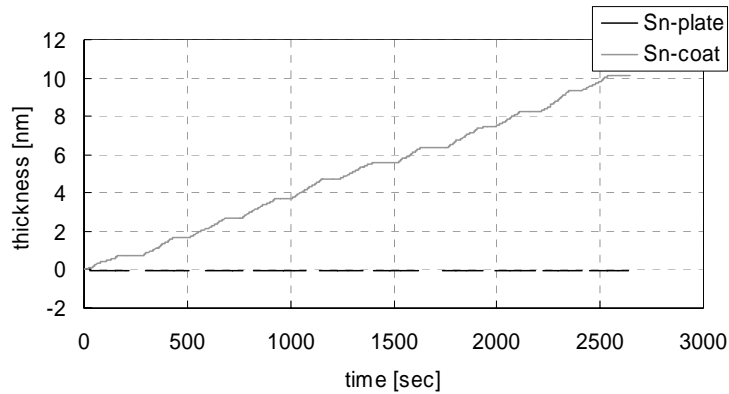


Fig.12. QCM result for a Sn-plate and a 800nm Sn coated glass substrate.

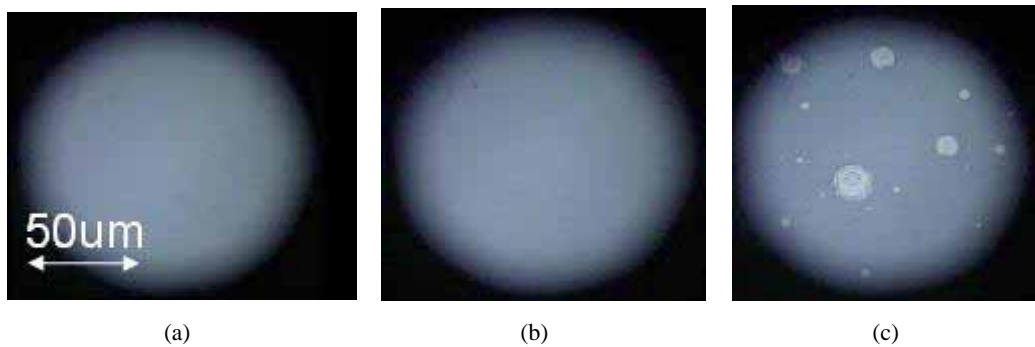


Fig.13. Optical microscope images of the Si witness plates: (a) without exposure, (b) Sn-plate target, (c) Sn coated glass target

## 4. DISCUSSION

We measured a dramatically reduced Sn deposition rate for a CO<sub>2</sub> drive laser as compared to a Nd:YAG laser which is probably due to a reduction of molten debris droplets. We consider the following generation mechanism for the molten debris:

During the plasma formation, the bulk target material is heated to sufficiently high temperatures to melt and vaporize. The molten material is then expelled, for example, by the plasma pressure and by generated shock (blast) waves. The ejected amount depends on the thickness of the molten layer, its viscosity and the plasma pressure.<sup>7</sup> For a reduction of the molten droplet debris, it is therefore important to suppress the molten layer and the plasma pressure, which, in addition, also does not contribute to EUV generation.

The critical density of a fundamental Nd:YAG laser is 100 times higher than the critical density of a CO<sub>2</sub> laser. It is therefore expected that the Nd:YAG laser produced plasma includes not only the optimum-temperature plasma region which efficiently generates EUV radiation, but also high density regions with temperatures, that do not generate EUV radiation but are the heat source for the generation of molten layers. In addition, the Nd:YAG plasma pressure is 100 times higher than the CO<sub>2</sub> laser plasma pressure at same temperature due to the different plasma density.

For a CO<sub>2</sub> laser produced plasma, on the other hand, these high density regions are much smaller resulting in reduced molten layers. In fact, the measured CE of the CO<sub>2</sub> laser produced plasma is larger than the CE of the Nd:YAG laser produced plasma, and the generated debris is respectively much smaller.

A magnetic field of 1T reduced the ion signal, i.e. the erosion, of a Nd:YAG laser generated plasma by more than 3 orders of magnitude. The deposition rate, on the other hand, did not change. We conclude from our experimental results that the influence of the ions on deposition is below 1%. For the CO<sub>2</sub> laser, however, the observed sputtering rate is higher than the deposition rate. Since the generated ion number is approximately equal to the amount of debris, (the observed erosion rate is close to zero) it can be concluded that the amount of debris is 1% or less as compared with the Nd:YAG laser.

In case of (average) erosion, it is possible, however, that very small debris particles form very thin Sn film areas on the mirror surface. Therefore, more detailed surface analysis is necessary.

## 5. CONCLUSION

Basic evaluation of debris and ion generation from a Sn plate irradiated with a CO<sub>2</sub> laser and a Nd:YAG laser was performed with several QCMs and Faraday cups. We observed erosion for the CO<sub>2</sub> drive laser and deposition for the Nd:YAG drive laser. A largely different amount of molten debris is the reason for this observation.

In **addition**, several Sn coated targets with different Sn thickness were investigated with respect to the generated debris for the CO<sub>2</sub> laser. We confirmed a mass limiting effect by the evaluation of these Sn targets. The main difference, however, was observed between the bulk Sn target and the coated Sn targets. Especially, the measured deposition for a 100nm Sn coated glass target is larger than for the bulk Sn target. This observation is related to a larger melted diameter on the target surface for the coated target. Differences in thermal conductivity, shock (blast)wave generation and/or adhesion are most probable reasons for this observation. In the future, more sensitive analysis has to be done in order to confirm the increased mirror lifetime expectation.

## ACKNOWLEDGEMENTS

Part of this work was done in collaboration with the Institute of Laser Engineering (ILE), Osaka University, and the authors greatly acknowledge the support by K.Nishihara, K.Nagai, S.Fujioka, Y.Izawa, and K.Mima from ILE. The authors also thank Y.Nishimura of Toyota Technical Development Corporation (TTDC) for the fabrication of the Sn coated Cu tape targets. The authors are deeply indebted to T.Higashiguchi (Department of Energy and Environmental Science, Graduate School of Engineering, Utsunomiya University) for many helpful discussions. Finally the authors thank Y.Wada from EUVA for his valuable technical support.

This work was performed under the management of the Extreme Ultraviolet Lithography System Development Association (EUVA), a research and development program of the New Energy and Industrial Technology Development Organization (NEDO), Japan.

## REFERENCES

1. Akira Endo, Hideo Hoshino, Tatsuya Ariga, Taisuke Miura, Yoshifumi Ueno, Masaki Nakano, Hiroshi Komori, Georg Soumagne, Hakaru Mizoguchi, Akira Sumitani, Koichi Toyoda, "Development Status of HVM Laser Produced Plasma EUV Light Source" Proc. Int.Sematech EUVL Symposium, Barcelona (2006).
2. Yoshifumi Ueno\*, Georg Soumagne, Hiroshi Komori, Takashi Suganuma, Akira Sumitani, Akira Endo, "Development of Magnetic Field Ion Mitigation" SEMATECH EUV Source Workshop, Vancouver (2006)
3. F.Bijkerk, E.Louis, M.van der Wiel, E.Turcu, G.Tallents, and D.Batani, "Performance optimization of a high-repetition - rate KrF laser plasma x-ray source for microlithography," *J.X-Ray Sci. Technol.*3,133-151(1992).
4. G.D.Kubiak, D.A.Tichenor, M.E.Malinowski, R.H.Stulen, S.J.Haney, K.W.Berger, L.A.Brown, J.E.Bjorkholm, R.Freeman, W.M.Mansfield, D.M.Tennant, O.R.Wodd II, J.Bokor, T.E.Jewell, D.L.White, D.L.Windt, and W.K.Waskiewics, "Diffraction-limited soft x-ray projection lithography with a laser plasma source", *J.Vac.Sci.Technol.* B9,3184-3188 (1991)
5. G.D.Kubiak, K.W.Berger, S.J.Haney, P.D.Rockett, and J.A.Hunter, "Laser plasma sources for SXPL: production and mitigation of debris," in *Soft X-Ray Projection Lithography*, A.Hawryluk and R.Stulen, eds., Vol.18 of OSA Proceedings Series (Optical Society of America, Washington, D.C., 1993)
6. H.A.Bender, A.M.Eligon, D.O'Connell, and W.T.Silfvast, "Average velocity distribution measurements of target debris from a laser-produced plasma," in *Applications of Laser Plasma Radiation*, M.C.Richardson, ed., *Proc.Photo-Opt.In-strum. Eng.* 2015,113-117 (1994)
7. C.Korner, R.Mayerhofer, M.Hartmann, H.W.Bergmann, "Physical and material aspects in using visible laser pulses of nanosecond duration for ablation", *Appl. Phys. A* 63, 123-131 (1996)